DEVELOPING A THERMAL EXEMPTIONS RATIONALE FOR LOW-POWER TRANSMITTERS

M. Prishvin, L. Bibilashvili, R. Zaridze
Laboratory of Applied Electrodynamics, Tbilisi State University, Tbilisi, 0128, Georgia
Email: rzaridze@laetsu.org

Abstract

The objective of this paper is to analyze realistic exposure scenarios by means of numerical computations. Our aim is to determine and compare peak values of SAR and temperature rise for several types of antennas. This paper contains results obtained in terms of MMF/GSMA WP8 2008-2010 years' project. Numerical simulations were performed on a human model [1].

1. INTRODUCTION

The recent numerical simulations results of electromagnetic (EM) exposure on a human body by wireless transmitters are discussed in this paper. A large number of dipole, monopole, and planar antennas have been studied at different frequencies and different distances between the head and the mobile phone in order to quantify the SAR level produced in the human body. The aim of this paper is to present and discuss results numerical simulation results. During the calculations the focus was made on the peak values of 10g avg. SAR and temperature rise. The simulations were conducted using the proprietary program package, which was developed in the Laboratory of Applied Electrodynamics and Radio Physics – FDTDLab [2-4] in cooperation with Motorola Inc. (2002-2008). Validation of FDTDLab was proved for EM and thermal solvers using different ways [3, 4]. The software package was enhanced with several new features including the calculation of peak values in selected tissue regions and/or tissue, and, most importantly, the consideration of directional blood flow [5] in the tissue capillary and its effect on the spatial distribution of the temperature and temperature rise in the Human model [1].

In accordance with specific requirements our aim was to investigate EM exposure and determine peak SAR and temperature rise values in various scenarios without consideration of directional blood flow. The first task included: use of the Finite Difference Time Domain (FDTD) method and anatomically based human head models; computation the peak 1-g and 10-g averaged SAR [6-9] and the temperature rise in the tissue for canonical dipole antennas of

various length: λ/2, λ/4, λ/8 and at 300, 450, 900, 1450, 1900 and 2450, 3700 6000 MHz –and at distances of 5, 10 and 20 mm from the head model. Frequencies up to 1900 MHz are used in wireless communication devices. Although the higher frequencies are not widely used yet, they are planned to be used in near future for mobile communications.

The second task was examining the monopole antennas on 300 MHz and 1450 MHz. The third task consisted in studying the planar antennas. Peak 1g and 10g averaged SAR and the temperature increase in tissue has been calculated for Patch Antennas, PIFA, and IFA Antennas. Patch antenna has been studied at 3700 MHz, while PIFAs was studied at 1900, 3700, and 6000 MHz. IFA Antennas were simulated at 6000 MHz. The 1-g and 10-g averaged-SAR distributions were subsequently computed on the basis of the algorithm specified in IEEE C95.3-2002 standard (IEEE, 2002) (2002) [6-9].

2. MATERIALS AND METHODS

The simulations were conducted using the FDTD method. Temperature increase in tissue was simulated due to RF exposure from antennas placed at different distances from the head model. The EM and thermal coupled solver FDTDLab, developed at TSU [3, 4], was used. As it is shown in [4] the thermal solver is tested against an analytical solution for a simplified case. At the initial phase of the project various standard antenna and phantom orientations were simulated. Along with the SAR the conventional bio-heat model was used to compute the temperature rise. 1 mm discretization has been used for all thermal and EM calculations except for 6000 MHz. Due to the small wavelength at 6000 MHz 0.5 mm discretization has been used around the feed. A head without the shoulders and a hand has been used in calculations. Antenna was placed at *"d"* distance from the nearest point of the head. The position of the antenna remained intact at all times during the simulation. A sinusoidal wave signal has been used at corresponding frequency. At lower frequencies 20 dB convergence criterion was used, while at high frequencies it was 40 dB. Thus, the resultant peak temperature rises corresponded to the infinite time exposure. These factors altogether gave us an idealized model which allowed us to study the worse (with highest expected temperature rise) possible exposure scenario that can never actually take place in the real life. Although FDTDLab allowed temperature dependent thermal parameters, they were constant during the simulation time. It is well known that there are

two kinds of effects caused by the RF field: biological and thermal. The current study is focused on the thermal effects.

The Pennes bio-heat equation (1) has been used along with the boundary condition (2) to simulate thermal processes in tissue.

$$\rho \cdot C \frac{\partial T}{\partial t} = \vec{\nabla} K \vec{\nabla} T + \rho \cdot SAR + A - B \cdot (T - T_b) \tag{1}$$

$$K \frac{\partial T}{\partial n} = -h(T - T_a) \tag{2}$$

Where A is the metabolic coefficient, B is blood perfusion coefficient, SAR is the specific absorption rate. The integral representation (3) of equation (1) was used for the finite difference approximation.

$$\int_{t_n}^{t_{n+1}} dt \iiint_V \rho \cdot C \frac{\partial T}{\partial t} dV = -\int_{t_n}^{t_{n+1}} dt \iint_S \vec{G} d\vec{s} + \int_{t_n}^{t_{n+1}} dt \iiint_V \rho \cdot SAR * dV + \int_{t_n}^{t_{n+1}} dt \iiint_V A_0 * dV$$
$$- \int_{t_n}^{t_{n+1}} dt \iiint_V B \cdot (T - T_b) * dV \tag{3}$$

Where dV is the elementary volume, ds is the elementary surface, $\vec{G} = -K\vec{\nabla}T$ is the flow through the boundary of the volume. The boundary condition (2) in integral form transforms to

$$\vec{G} = -h(T - T_a) \tag{4}$$

In equation (4) T_a is the air temperature and h is the convection coefficient. For all calculations those parameters were h = 10.5 and T_a = 23 ºC. The simulation time step for all thermal calculations was dt = 0.5sec. All results have been normalized to 1W input power.

3. DIPOLE ANTENNAS

In terms of the MMF WP8 project the dipole antennas have been investigated at different frequencies and distances from the head model. Calculations have been conducted on all frequencies except 1900 MHz. Initially the MMF WP8 project tasks were divided between two collaborators. It was planned to submit a joint report with data obtained by two research groups. Later, due to discrepancies in approach to the calculations, separate papers have been submitted. Despite the fact that only calculations at 300, 450 1450 and 3700 MHz were planned to be

conducted in TSU, projects at 900, 2450 and 6000 MHz were also investigated in order to analyze frequency dependencies of SAR and temperature rise. These additional calculations helped in analysis of other antennas studied in terms of this project.

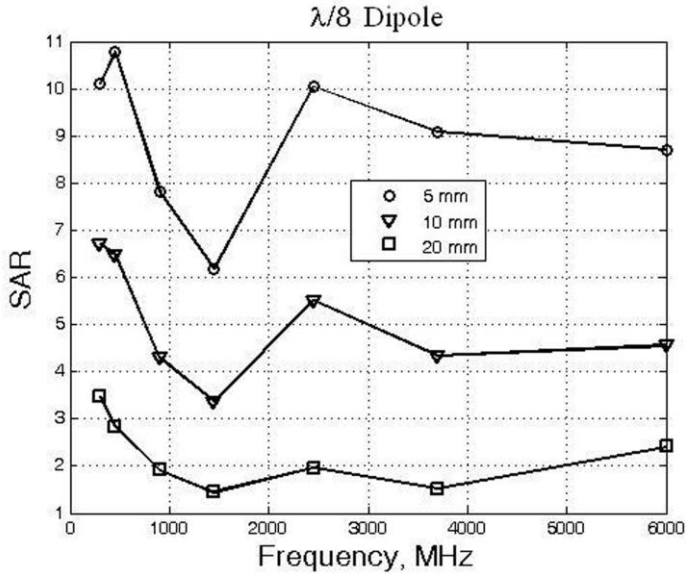

Fig.1 SAR on frequency. All data normalized to input power

Dependency of peak 10g SAR on frequency is presented on Fig. 1. As it can be seen the minimal 10g SAR is observed at 1450 MHz with a local peak at 2450 MHz, while the maximum is at lower frequencies. On the figure data for all of the separation distances, namely 5, 10 and 20mm, is presented. For all calculations peak values of avg. SAR decrease when the separation distance increases. The graphs for 5, 10 and 20mm have similar shape. It can be seen that the higher the distance is the smoother is the corresponding graph. The reason of this the radiation pattern of the antennas. With the increase of the separation distance the difference in radiation pattern for different frequencies is less notable. After the distribution of SAR has been obtained thermal calculations were conducted for each antenna project. The dependency of temperature rise on frequency for λ/8 dipole is presented on Fig. 2. The minimal temperature rise is observed at 900MHz. In most cases the peak temperature rise was located in the ear, thus the resultant temperature was less than 38ºC.

The maximal peak temperature rise for all calculations is at 6000 MHz and is located in the ear. It should be noted that at 6000 MHz results are not stable. A small change in the input parameters can significantly affect the resultant distributions.

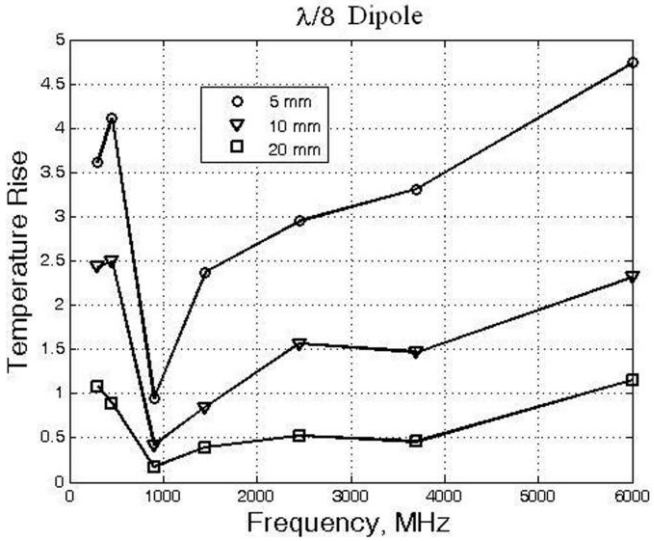

Fig. 2 Temperature rise on frequency. All data normalized to input power

The 10g SAR dependency on frequency for λ/4 dipoles is presented on Fig. 3. The minimal peak 10g SAR is observed at 300 MHz for all distances. At the same time from Fig. 4 we see that the minimal temperature rise for the same antennas is again found at 900 MHz. At low frequencies (300 and 450 MHz) field penetrate deep into the model.

The high values at lower frequencies for λ/8 dipole antennas can be explained by the resonant dimensions of the head model.

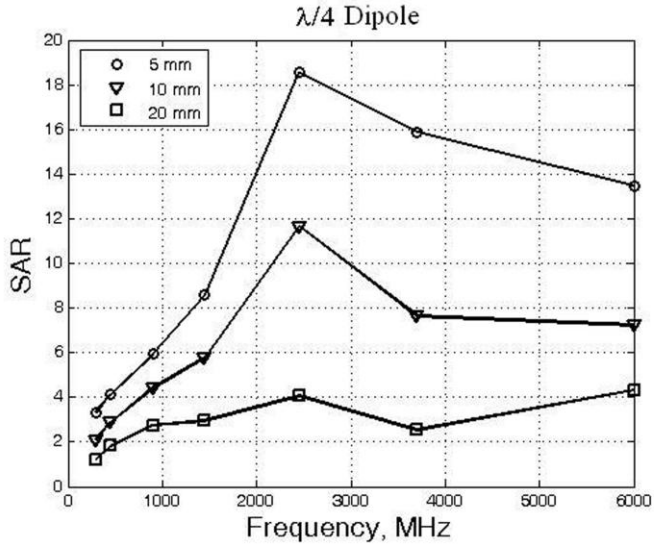

Fig. 3 SAR on temperature rise for λ /4 dipole antennas

It must be noted that the user's hand is not taken into account. Preliminary calculations show [11] that with the hand present the results are different, since it absorbs the energy and drastically changes the radiation pattern. The radiation pattern makes the placement of the antenna a subject of separate study. All examined scenarios represent an ideal case: an infinite exposure with the antenna at the same point. If the direction of a beam matches peculiarity of the model the induced temperature rise will be higher. But if the mobile handset is moved during the communication process the beam moves from one point of the model to another, resulting in much smaller peak values of SAR and temperature rise. The effect of changing position of the antenna should be studied in the future.

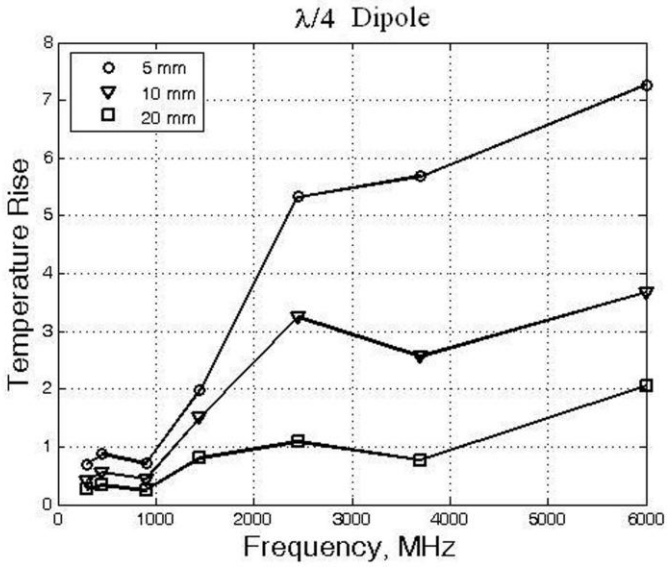

Fig.4 Temperature rise on frequencies for λ /4 dipole antennas

As it can be seen from Fig. 3 and Fig. 4 at lower frequencies the peak values are much lower for λ /4 dipole antennas. The cause of this is the difference in radiation pattern for the two cases (λ/4 and λ /8 dipole antennas). For the smaller antenna it (the radiation pattern) is more directed. The resultant peak values of SAR and temperature rise are higher when the beam's direction matches the peculiarity of the model. A local maximum is observed at 2450 MHz for both λ/4 and λ/8 dipole. At the same time the penetration depth at 2450 MHz is higher than at 3700 and up. The penetration depth depends on σ conductivity of the materials. The higher is the σ conductivity the smaller is the penetration depth of EM field. Dependencies of conductivity on frequency for muscle, skin and SAT are shown on Fig. 5. The conductivity determines the

penetration depth of EM field. As it can be seen from Fig. 5 the conductivity for higher frequencies can be 10 times higher than at low frequencies. That is the reason why field penetration depth is relatively small on high frequencies, while at low frequencies it is significantly higher.

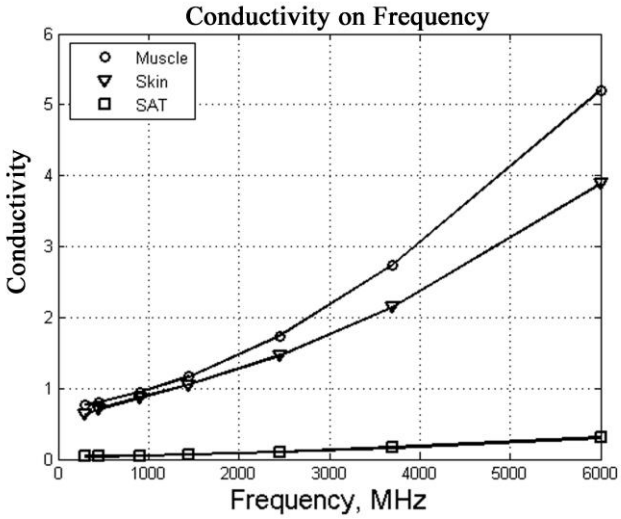

Fig. 5. Conductivity on frequency. At 6000 MHz σ conductivity is almost ten times higher than at 300MHz.

On Fig. 6 the distributions of 10g SAR and temperature rise are presented. As it can be seen from Fig. 6 location of peak temperature rise and SAR depend on particular case and may not correspond to each other. In this case match only locations of peak 1g SAR and temperature rise while the location of peak 10g SAR is in another part of the model. The geometry of the antenna and its placement can drastically affect resultant distributions of SAR and temperature rise.

a) b)

Fig. 6. Locations of peak a) 10g SAR = 6.7w/kg b) temperature rise ΔT=0.36°C of λ/8-th Dipole Antenna for frequency 300 MHz, at 10 mm distance.

In some cases, when the field penetration depth is comparable with the linear dimensions of the model, a focusing effect can be observed Fig. 7. Due to complexity of the model and frequency dependent material properties, points of maximal SAR and temperature rise are located in different parts of the head and may not correspond to each other (Fig.6). As a result, graphs are not smooth and it is harder to make conclusions based on them.

Field penetration depth is significantly bigger at low frequencies Fig. 7. Values of SAR and temperature rise for inner parts of the model (e.g. brain, eye, etc.) are much higher for lower frequencies. Starting from 1450 MHz the penetration depth of EM field is small and biggest part of radiated energy is absorbed at the surface, which in the studied model in most cases is the ear. If the position of device is changed during the communication process, the peak values are washed out and the impact is be smaller.

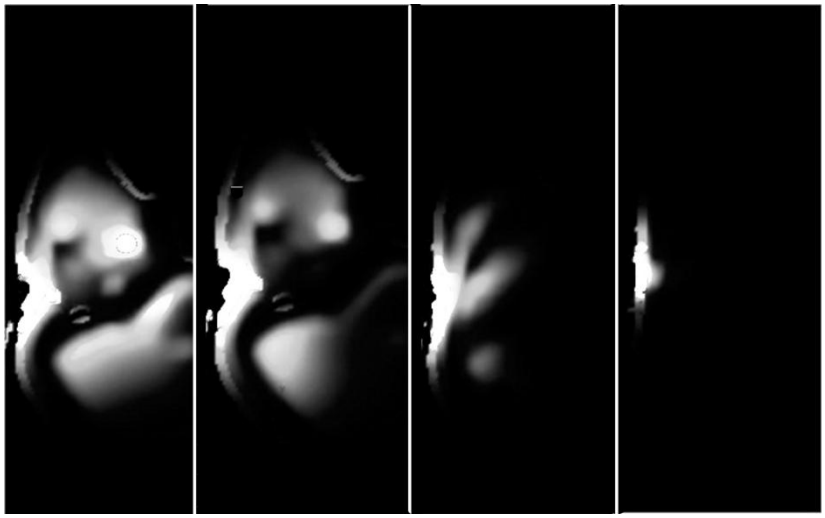

a) b) c) d)

Fig. 7. Field penetration depth for λ/2-th dipole antennas. 1g SAR with frequencies:
a) 300 MHz b) 450 MHz c) 1450 MHz and d) 3700 MHz

From Fig. 8 it can be seen that there is a good correlation between SAR and temperature rise for dipole antennas. It turned out that the correlation depends on the dipole length. When the correlation was calculated based on all simulation results together (λ/2, λ/4, λ/8, λ/15 dipoles) it appeared that R2=0.73. At the same time for λ/2, λ/4, λ/8 dipole antennas R2=0.91 (Fig. 8) and for λ/15 antennas apart it is R2=0.93. This fact is explained as follows.

The λ/15 dipole antennas are smaller and their radiation pattern is more directed compared to the bigger antennas. In such cases the point SAR appeared to be concentrated in a smaller area. Considering that the boundary conditions are the same the heat flow through the boundary is smaller. As a result for such cases the temperature rise values are higher. Overall good correlation is observed for all calculations.

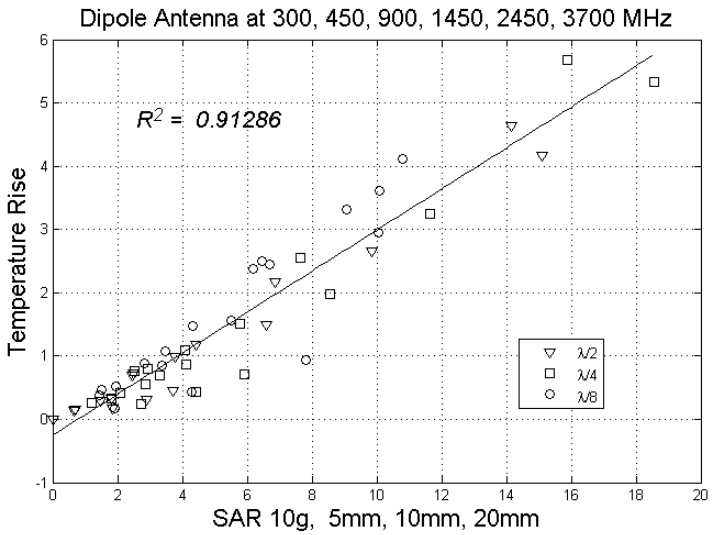

Fig. 8 Correlation of 10g avg. SAR and temperature rise.

4. MONOPOLE ANTENNAS

Resonant λ/4 monopole antennas operating at (300 and 1450) MHz were investigated in terms of MMF WP8 project. The temperature rise and SAR were the subject of study in all calculations. Antennas were placed at distances of 10 and 20 mm from the Duke Head model [1].

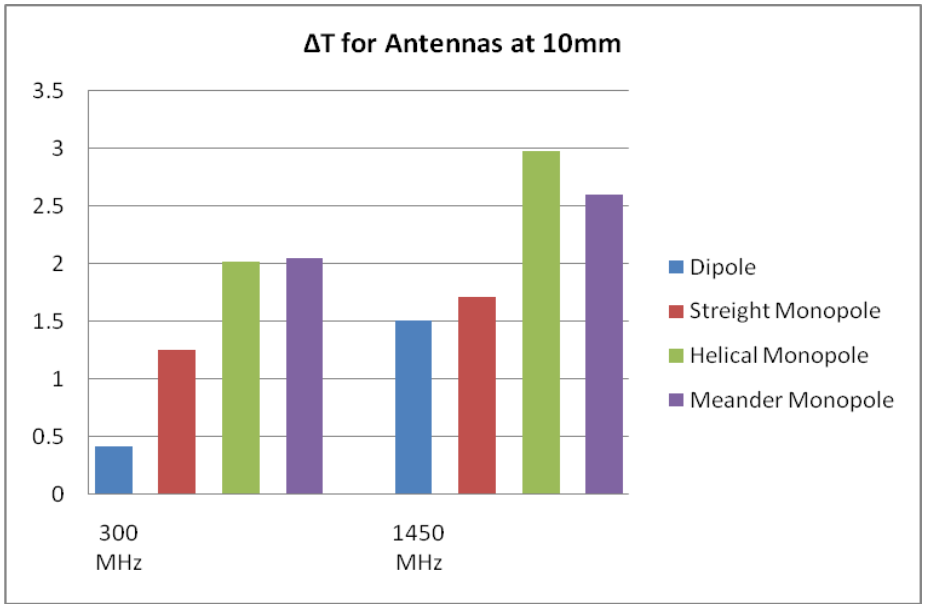

Fig. 9 Temperature Rise for Antennas at 10mm, 300MHz and 1450 Mhz

Three types of monopoles namely; the straight, the helical and the meander were mounted on top of a metal box. A 1 mm uniform discretization was used for all calculations. Each monopole was excited using a 1 mm excitation gap with a continuous wave sinusoidal source at a given frequency. All SAR and temperature rise data were normalized to 1W of power. On Fig. 9 temperature rise for monopole antennas is compared to temperature rise of a dipole antenna of the same length. At 10mm distance the dipole antenna induced the smallest temperature rise at both frequencies. As it has been shown for dipoles, both SAR and temperature values decrease with the increase of distance. Since tissue thermal parameters like specific heat, heat conductivity, blood perfusion etc. are independent of frequency the temperature rise depends only on the point SAR.

The maximal temperature rise $\Delta T=2.97$ °C and maximal 10g SAR=10.5 W/kg were observed in the earlobe at 1450 MHz for 10mm helical monopole. The resultant maximal temperature did not exceed 37°C.

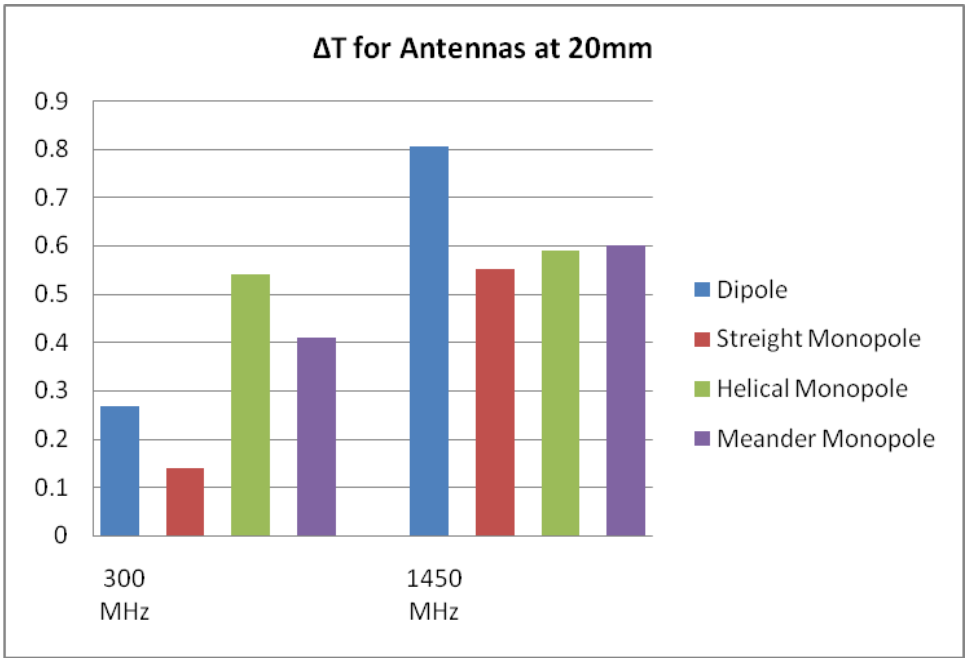

Fig. 10 Temperature Rise for Antennas at 10mm, 300MHz and 1450 Mhz

The minimal temperature rise ΔT=0.14°C was observed at 300 MHz. Minimal peak 10g SAR was observed at 300 MHz for straight monopole located at 20mm distance from the model. Temperature rise and SAR for the same antenna types are lower at 300 MHz and higher at 1450 MHz. This fact is caused mostly by the penetration depth, which is much smaller at higher frequencies. At 1450 MHz energy is absorbed at the surface and the peak values of temperature rise are located mostly in the ear, while at 300 MHz they may be located in the head tissues. As expected peak values of temperature rise are much lower at 20mm distance.

At 300 MHz, 20mm the smallest temperature rise is induced by the straight monopole. At 1450 MHz all monopole antennas are very close to each other with smaller temperature rise compared to the dipole at the same frequency. The difference in temperature rise between dipole and monopole antennas of the same length is caused by the radiation pattern and antenna placement.

5. PIFA ANTENNAS

Planar inverted-F antennas (PIFA) operating at, 1900, 3700, and 6000 MHz were investigated 10 and 20 mm distances from the Duke head model. Two different orientations of the PIFA namely the “conventional” and the “flipped” were used. In the conventional orientation the gap

was placed on the outer surface of a metal box, while in the "flipped" it was on the inner surface (directed towards the head model).

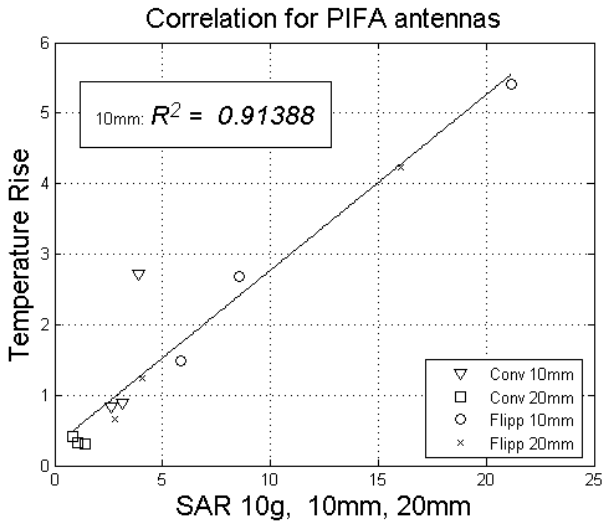

Fig. 11. Correlation between 10g SAR and temperature rise at 1900, 3700, 6000 frequencies.

PIFA Antennas have been simulated at 1900, 3700 and 6000 MHz. The distance *„d"* is calculated as the separation between the outer edge of the compressed ear and the surface of the metal box facing the metal strip of the PIFA antenna. The time step for thermal calculations was 0.5 second for all antennas. The basal body temperature was considered as 37˚C while the air at was 23˚C.

The maximal temperature rise ΔT=4.68°C and maximal 10g SAR = 8.41 W/kg were observed at 6000 MHz 10mm PIFA antenna with flipped orientation. The minimal temperature rise ΔT=0.21°C was observed at 1900MHz for PIFA antenna with conventional orientation located at 20mm distance from the model.

Good correlation between SAR and temperature rise was observed at all frequencies. Although the temperature rise of 4.68 °C is high enough, the resultant maximal temperature does not exceed 38°C. While conducting the calculations it was noted that antenna position may drastically affect resultant peak values of SAR and temperature rise and corresponding distributions.

The maximum ΔT exhibits a strong correlation with both peak 1-g avg. SAR and peak 10-g avg. SAR. Fig. 11 shows the peak ΔT values for the 1900, 3700 and 6000 MHz PIFAs plotted against the 10-g avg. SAR. Similar dependency is observed for 1g SAR. [10-12].

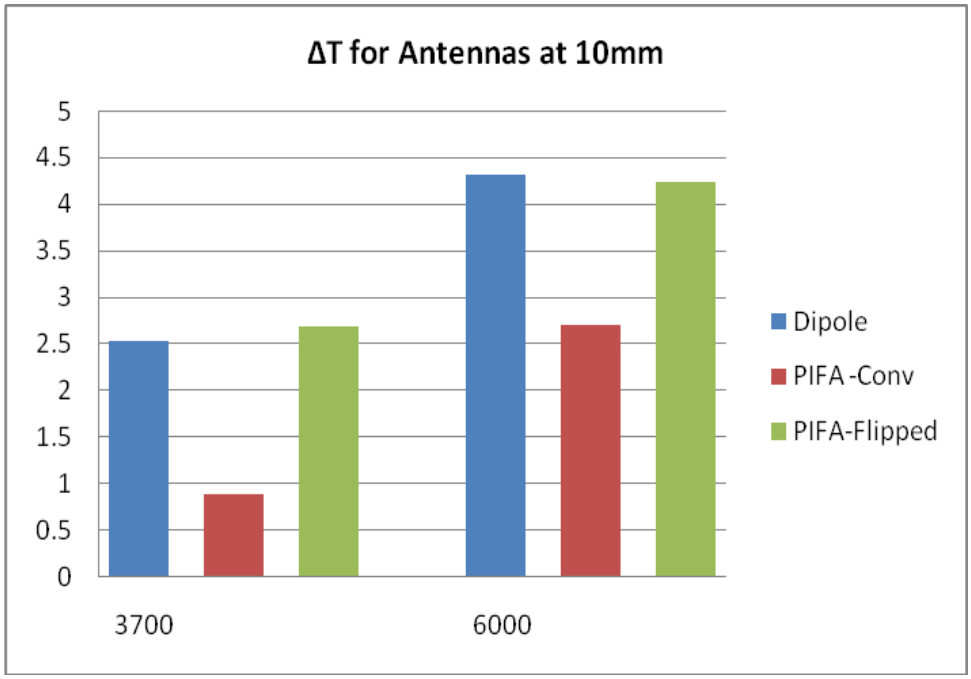

Fig. 12 Temperature Rise for Antennas at 3700 and 6000 MHz.

The more precise analysis can be made according to Fig. 12. It can be seen that PIFA antennas with "flipped" orientation induct significantly higher temperature rise compared to the "conventional" orientation. The same conclusion is true for 20mm distance.

For all simulations peak values of temperature rise at 3700 MHz are lower than at 6000 MHz. As for 10 mm distance, the peak temperatre values for "flipped" PIFA antenna are signifacntly higher compared to the "conventional" orientation. The peak values of temperature rise of PIFA antennas with "flipped" orientation are very close to the peak values for dipole antennas.

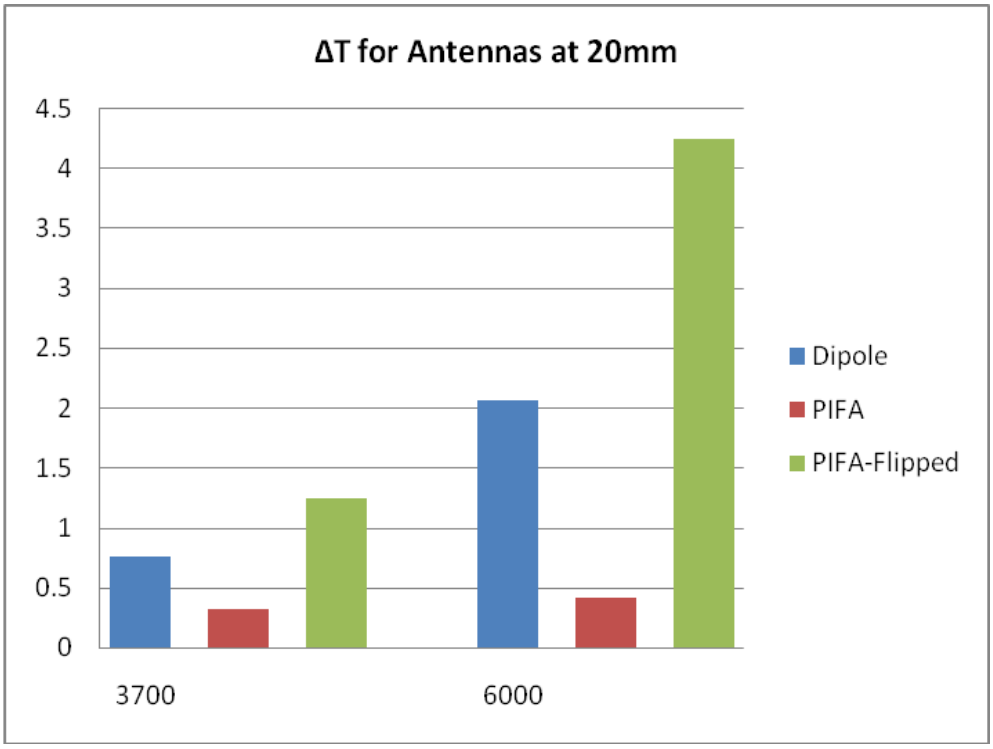

Fig. 13. Temperature Rise for Antennas at 20mm, 3700 and 6000 MHz.

At 20 mm distance the peak temperature rise values for dipole and "flipped" PIFA antennas are not close any more. This is due to the resonant distances between the PIFA anetnna model and the head model. This fact is explained more detailed later in this article.

6. PATCH ANTENNAS.

Patch antennas have been investigated at 3700 MHz. Two separation distances namely 10 and 20mm were used.

The patch antennas appeared to be very similar to the PIFA antennas. The same conclusions that were made for the PIFA antennas can be applied to them. The peak values of SAR and temperature rise for "flipped" orientation is much higher compared to the "conventional" orientation. At the same time the values for the "flipped" orientation are close to dipole. At 20 mm distance the temperature rise is times smaller compared to the 10mm distanfce. The peak temperature rises were located in the ear tissues for all calculations.

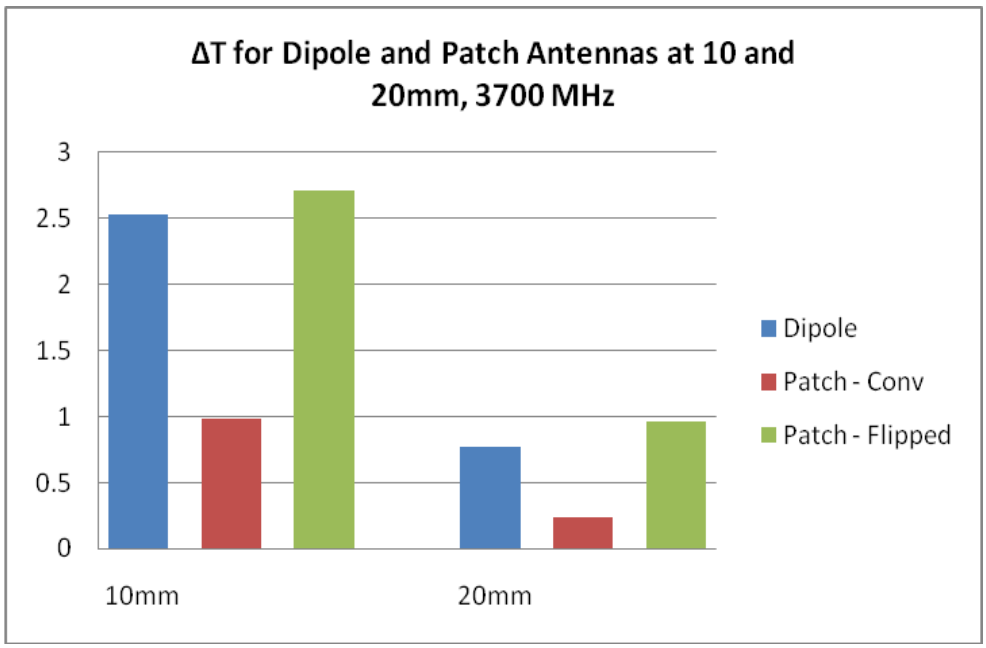

Fig. 14 Temperature rise for Dipole and Patch antennas at 3700 MHz.

7. IFA ANTENNAS

Data, obtained for IFA (inverted-F antenna) antennas, is provided in table 1.

Table 1. Data for IFA antenna operating at 6000 MHz, all data normalized to 1W input power.

6000 MHz	10 mm			20 mm		
	1g SAR	10g SAR	ΔT	1g SAR	10g SAR	ΔT
Conventional	24.8	4.77	3.01	11.21	2.56	1.45
Flipped	53.1	12.66	6.37	63.88	16.97	**7.78**

Like it has been observed for Patch and PIFA antennas IFA antennas induce much higher temperature rise in flipped position compared to "conventioanal" one. In conventional orientation for IFA antennas the temperature rise is bigger at 10mm and smaller at 20mm distances. But the situation changes at 20mm. An unexpected behavior has been observed for 6000 MHz "flipped" IFA antenna at 20mm. The peak SAR and temperature rise values appeared to be higher than at 10mm. This case has been investigated in detail. The wave length at 6000 MHz is around 5cm, the distance from the antenna to the nearest point of the model is 2cm. It appeared that the IFA "antenna-head" model is resonant. The resonance had caused an

unexpected high temperature rise at 20mm distance. The resonance phenomena for RF exposure simulations is a subject of a separate study.

8. CONCLUSION

Thermal impacts of dipole, monopole, planar and patch antennas operating at several frequencies were investigated. Peak values of specific absorption rate (SAR) and induced temperature rise in the Duke Head model were presented. All of examined antennas have been compared to dipole antennas. The position of the antenna remained intact at all times during the simulation time. A sinusoidal wave signal has been used at corresponding frequency. Thus, the resultant peak values of SAR and temperature rise corresponded to the infinite time exposure and, therefore, obtained values were much higher than they would have been in reality.

Following conclusions were made:

1. The smallest temperature rise appeared to be at 900MHz and 1 900MHz (Fig. 1, 2).
2. Peak temperature rise ranged from 0.1˚C to 7.78˚C for all the antennas considered. Cases with high temperature rise values were investigated separately. The wave length at 6000 MHz is about 5cm. At this frequency the distances between the antenna and the ear, the antenna and the head are resonant. In case, when a resonance takes place, the resultant temperature rises are above normal.
3. Due to the frequency dependant absorption of tissues (see Fig. 5.) the high temperature rise values observed at high frequencies are located in the tissues of the model (Fig 7. d) and the maximal temperature in the model does not exceed 38˚C for most cases.
4. At lower frequencies the penetration depth is high, and studied model has been observed to focus EM filed, concentrating RF energy in some local points inside of the model (see Fig. 7). The hot spots appeared in the brain. Detailed studies show, that their position shifts when the antenna placement is changed. Their dimensions and location depend on the curvature of the head's surface. The subject of big interest is the investigation of the focusing effect on the model of a child.
5. Overall a good correlation between 10g SAR and temperature rise was observed (Fig.8 and Fig. 11)

6. Due to asymmetrical radiation pattern monopole antennas in most cases inducted higher temperature rise compared to the dipole antennas (see Fig. 9). But overall they are identical to dipole antennas and peak temperature rise and SAR values are determined mostly by the antenna placement.
7. Planar antennas with the flipped orientation induced much higher temperature rise than in the conventional.
8. It has been shown that planar antennas with "flipped" orientation are very similar to dipole antennas.
9. A local maximum of temperature rise is observed at 2450 MHz. At this frequency the penetration depth is higher than at 3700 MHz and up. Probably this is the reason why the microwave heaters work at this frequency. It is known that the presence of the high permittivity and conductivity dielectric changes the radiation pattern and the dielectric absorbs the most part of radiated energy. From our point of view, the use of high frequencies is not recommended because of the high absorption at them.
10. Preliminary calculations show [11] that the presence of a hand affects the radiation pattern. The hand redirects the radiated EM field's energy along itself and peak temperature rise values in the head are drastically reduced. From our point of view this topic must be investigated more carefully.
11. Due to the directed radiation pattern of some antennas, it has been noticed that their placement also affects the temperature rise. The placement of the antenna is a subject of study.
12. A resonance has been observed for IFA antenna at 20mm. The resonance was the cause of the unexpectedly high temperature rise (see Table 1).
13. IFA antennas induce higher temperature rise compared to Patch and PIFA antennas. A resonance has been observed for "flipped" IFA antenna at 20mm.
14. At 6000MHz results are not stable. A small change in the input parameters can significantly affect the resultant distributions.

ACKNOWLEDGEMENT

This work was supported by the Mobile Manufacturers Forum (MMF), Belgium & Hong Kong and the GSM Association (GSMA), London, UK.

REFERENCES

[1]. N. Kuster. IT'IS Foundation. http://www.itis.ethz.ch/

[2]. Bijamov, A. Razmadze, L. Shoshiashvili, R. Zaridze, G. Bit-Babik, A. Faraone, "Software for the electro-thermal simulation of the human exposed to the mobile antenna radiation", Proceedings of VIII-th International Seminar/Workshop on Direct and Inverse Problems of Electromagnetic and Acustic Wave Theory (DIPED-2003), Lviv, Ukraine, September 23-25, 2003, pp.173-176. http://www.ewh.ieee.org/soc/cpmt/ukraine/

[3]. R. Zaridze, N. Gritsenko, G. Kajaia, E. Nikolaeva, A. Razmadze, L. Shoshiashvili, A. Bijamov, G. Bit-Babik, A. Faraone, "Electro-Thermal Computational Suit for Investigation of RF Power Absorption and Associated Temperature Change in Human Body", 2005 IEEE AP-S International Symposium and USNC/URSI National Radio Science Meeting, July 3-8, 2005, Washington DC, USA. p. 175-178

[4]. L. Shoshiashvili, A. Razmadze, N. Jejelava, R. Zaridze, G. Bit-Babik, A. Faraone. "Validation of numerical bioheat FDTD model". Proceedings of XI-th International Seminar/Workshop on Direct and Inverse Problems of Electromagnetic and Acoustic Wave Theory (DIPED-2006), October 11-13, 2006, Tbilisi, Georgia. pp. 201-204.

[5]. Mikheil Prishvin, Liana Manukyan, Revaz Zaridze. "Vascular Structure Model for Improved Numerical Simulation of Heat Transfer in Human Tissue", 20-th International Zurich Symposium on Electromagnetic Compatibility, January 12-16 2009, Zurich, Switzerland. pp. 261-264

[6]. Md. R. Islam, Alex Razmadze, Revaz Zaridze, Giorgi Bit-Babik, and M. Ali, "Computed SAR and Temperature Rise in an Anatomical Head Model by Canonical Antennas", BEMS Annual Meeting, BEMS-2009 Congress Centre, Davos, Switzerland, June 14 - 19, 2009, http://bioem2009.org/technical-program/.

[7]. R. Zaridze, A. Razmadze, L. Shoshiashvili, D. Kakulia, G. Bit-Babik, A. Faraone. Influence of SAR Averaging Schemes on the Correlation with Temperature Rise in the 30-800 MHz

Range. EUROEM 2008 European Electromagnetics, 21-25 July 2008, Swiss Federal Institute of Technology (EPFL), Lausanne, Switzerland. pp.120

[8]. Bernardi et al. “Specific Absorption Rate and Temperature Increases in the Head of a Cellular-Phone User,” IEEE Trans. Microwave Theory Tech., vol.48, no.7, pp. 1118-1126, July 2000.

[9]. A. Razmadze, L. Shoshiashvili, D. Kakulia, R. Zaridze, "Influence on averaging masses on correlation between mass-averaged SAR and temperature rise". Journal of Applied Electromagnetism, vol.10, no 2. December 2008. pp. 8-21. http://jae.ece.ntua.gr/JAE December 2008/SAR and temperature rise Zaridze Paper 2.doc.pdf

[10]. D. Mazmanov, L. Manukyan, D. Kakulia, A. Razmadze, L. Shoshiashvili, R. Zaridze. MAS based software for the solving of diffraction and SAR problems on unbounded objects. Proceedings of XI-th International Seminar/Workshop on Direct and Inverse Problems of Electromagnetic and Acoustic Wave Theory (DIPED-2006), October 11-13, 2006, Tbilisi, Georgia. pp. 11-16

[11]. R. Zaridze, M. Prishvin, V. Tabatadze, D. Kakulia, "Hand Position Effect on SAR and Antenna Pattern in RF Exposure Study of a Human Head Model" BEMS-2009 Congress Centre, Davos, Technical Program, Switzerland, June 14 - 19, 2009, http://bioem2009.org/technical-program